

A Satellite Cross-Calibration Experiment

Jens Nieke, Teruo Aoki, Tomonori Tanikawa, Hiroki Motoyoshi, and Masahiro Hori

Abstract—Recently, the Advanced Earth Observing Satellite 2 (ADEOS-2) was launched (December 14, 2002) successfully, and the Global Imager (GLI) onboard the ADEOS-2 satellite became operational in April 2003. In a first calibration checkup, the radiometric performance of GLI was compared relatively to that of other sensors on different satellites with different calibration backgrounds. As a calibration site, a large snowfield near Barrow, AK, was used, where space sensors in polar orbits view the same ground target on the same day with small differences in the local crossing times. This is why GLI, the Moderate Resolution Imaging Spectroradiometer (Terra, Aqua), the Sea-viewing Wide Field-of-view Sensor, the Advanced Very High Resolution Radiometer (N16, N17), the Medium Resolution Imaging Spectrometer, and the Advanced Along Track Scanning Radiometer datasets were selected for the following clear-sky condition days: April 14 and 26, 2003. At the same time, ground-truth experiments (e.g., measurements of ground reflectance, bidirectional reflectance distribution function, aerosol optical thickness) were carried out. Thereinafter, top-of-atmosphere (TOA) radiance/reflectance was forward calculated by means of radiative transfer code for each sensor, each band, and each day. Finally, the vicariously retrieved TOA signal was compared to TOA sensor Level 1B data. As a result, GLI's performance is encouraging at that time of the mission. GLI and the other seven sensors deliver similar sensor output in the range of about 5% to 7% around the expected vicariously calculated TOA signal.

Index Terms—Advanced Along Track Scanning Radiometer (AATSR), Advanced Very High Resolution Radiometer (AVHRR), Global Imager (GLI), intersatellite calibration, Medium Resolution Imaging Spectrometer (MERIS), Moderate Resolution Imaging Spectroradiometer (MODIS), Sea-viewing Wide Field-of-view Sensor (SeaWiFS), vicarious calibration.

I. INTRODUCTION

THE MULTICHANNEL optical whiskbroom scanner Global Imager (GLI) [1] (see also <http://sharaku.eorc.nasda.go.jp/GLI/>) was launched successfully on the Advanced Earth Observing Satellite 2 (ADEOS-2) in December 2002. GLI provided highly needed data of the earth's surface in the spectral region from 0.38–12 μm for a better understanding of the environment in global and regional scale. From Table I, the main specifications of GLI can be depicted.

Manuscript received August 13, 2003; revised February 15, 2004.

J. Nieke is with the Remote Sensing Laboratories, University of Zürich, CH-8057 Zürich, Switzerland (e-mail: nieke@geo.unizh.ch).

T. Aoki is with the Meteorological Research Institute, Meteorological Agency (JMA), Tsukuba 305-0052, Japan (e-mail: teaoki@mri-jma.go.jp).

T. Tanikawa is with the Graduate School of Life and Environmental Sciences, University of Tsukuba, Tsukuba 305-8572, Japan (e-mail: tanikawa@atm.geo.tsukuba.ac.jp).

H. Motoyoshi is with the Space Service, Tsukuba 305-0028, Japan (e-mail: hmotoyos@mri-jma.go.jp).

M. Hori is with the Earth Observation Research and Application Center (EORC), Japan Aerospace Exploration Agency, Tokyo 104-6023, Japan (e-mail: nori@eorc.nasda.go.jp).

Digital Object Identifier 10.1109/LGRS.2004.831202

TABLE I
MAIN SPECIFICATIONS OF GLI

| Parameter | Value |
|------------------------------------|---|
| Launch | Dec. 2002 on ADEOS-2 |
| Spectral range | 375 nm – 12.5 μm |
| Number of spectral bands | 36 |
| Spectral bandwidth | 10 nm (VNIR / 1 km) |
| Instantaneous field of view (IFOV) | 1.25 mrad (1 km) or 312.5 μrad (250 m) at nadir |
| Scanning angle | $\pm 45^\circ$; swath = 1600 km |
| Quantization | 12 bit |
| Tilt angle (across track) | -18.5° , 0° , 18.5° |
| Mass | 475 kg |
| Calibration (on-board) | VNIR, SWIR: Solar and lamp MTIR: black body, deep space |

Earth observation data require a careful calibration of the sensor and validation of the algorithms to demonstrate the reliability of the data products at the required accuracy, such as described in [2]. Consequently, the calibration of the GLI is one of the key parts in the sensor design, and efforts are made to check the sensor before launch (prelaunch calibration) and during mission duration time (onboard and vicarious and cross-calibration methods). From launch until the failure of the ADEOS-2 satellite (October 24, 2003), GLI was in the calibration and validation (CalVal) phase. In the CalVal phase, which generally ends 12 months after launch, the sensor output has to be checked rigorously using different CalVal techniques before the GLI data will be made available to the remote sensing user community. Besides onboard (e.g., solar, lamp, blackbody) and vicarious (e.g., desert sites, ocean sites) calibration, the comparison with other space sensors delivers a better understanding of GLI's performance. In the following, an approach is described to make use of simultaneous observations of space sensors on different satellites combined with ground-truth experiments performed during the satellites overflights. The selected space sensors have some similarity with GLI in respect of the spectral, spatial, and radiometric characteristics. These sensors were observing almost at the same time a ground target, where simultaneous ground-truth measurements are performed.

The capability of this cross-calibration approach over snowfields has been demonstrated recently in a case study for a Sea-viewing Wide Field-of-view Sensor (SeaWiFS)–Medium Resolution Imaging Spectrometer (MERIS) intercomparison [3]. At that time, only ground-truth data were taken into account, which describe the atmospheric conditions.

In this letter, the cross-calibration approach was improved by performing additional ground-truth reflectance measurements. For April 14 and 26, 2003, GLI Level 1B (L1B) datasets were successfully compared with L1B datasets of the Moderate Resolution Imaging Spectroradiometer (MODIS) (Terra, Aqua), SeaWiFS, the Advanced Very High Resolution Radiometer (AVHRR) (N16, N17), MERIS, and the Advanced Along Track Scanning Radiometer (AATSR) over a large snowfield close

to Barrow, AK. At the same time, a ground-truth campaign at Barrow delivered a good *in situ* site description during the overflights of the satellites.

II. GROUND-TRUTH EXPERIMENT AT BARROW (APRIL 14/26, 2003)

A. Basic Approach

The datasets from different sensors, such as GLI, MODIS, SeaWiFS, AVHRR (N16, N17), and MERIS/AATSR were used for this intercomparison. These sensors are onboard different spacecrafts (ADEOS-2, Terra, Aqua, ENVISAT, Orbview-2/SeaStar, NOAA-16, NOAA-17) and passed the CalVal site at Barrow at least once during the ongoing ground-truth experiment. During the ground-truth campaign, various measurements were carried out, such as (bidirectional) spectral ground reflectance and aerosol optical thickness (AOT) measurements.

Both ground and satellite data were input data in a radiance transfer code (RTC), as RTC, a slightly modified version of the 6S code [4], was used. The modifications in the 6S code consist mainly of supplementary subroutines to account for updated solar irradiance [5] and spectral response functions, such as those of the above-mentioned space sensors.

Using the ground-truth data, the top-of-atmosphere (TOA) radiance and reflectance for each sensor and each channel were calculated forwardly for each overpass. The resulting calculated TOA data were compared with the measured satellite sensor data.

B. Satellite Data

Satellite sensor data of the following seven space sensors were intercompared:

- 1) GLI onboard ADEOS-2; prelaunch calibrated (launched December 2002);
- 2) MODIS onboard Terra; operational L1B TOA reflectance/radiance data (launched December 1999);
- 3) MODIS onboard Aqua; operational L1B TOA reflectance/radiance (launched May 2002);
- 4) AVHRR/3 onboard NOAA-16; L1B using MODIS-based calibration coefficients [6] (launched September 2000);
- 5) SeaWiFS onboard Orbview-2/SeaStar; L1B retrieved from L1A with SeaDAS 4.4 (launched August 1997);
- 6) AVHRR/3 onboard NOAA-17; prelaunch calibration (launched May 2002);
- 7) MERIS and AATSR onboard ENVISAT; operational L1B TOA radiance/reflectance (launched March 2002).

Table II gives an overview on the spectral characteristics of the sensors, such as center wavelength and spectral bandwidth.

C. Geometric Information

In Tables III and IV, the successive passing times (all in UTC) can be depicted for the satellite crossing at Barrow on April 14/26, 2003. In the following, the period from 22:35–23:33 (14th) and 21:41–23:19 (26th) was selected. Unfortunately, there was no MODIS (Terra) dataset available for April 14, same for the April 26 SeaWiFS dataset. On April 14, 2003,

TABLE II
SPECTRAL CHARACTERISTICS OF SPACE SENSOR DATA
USED IN THIS CROSS CALIBRATION

| Sensor | GLI | | SeaWiFS | | MERIS | | MODIS | | AATSR | | AVHRR | | |
|-------------------|---------------------|-------------------------|---------------------|-------------------------|---------------------|-------------------------|---------------------|-------------------------|---------------------|-------------------------|---------------------|-------------------------|--|
| Satellite | ADEOS-2 | | Orbview-2 | | ENVISAT | | Aqua, Terra | | ENVISAT | | N-16, N-17 | | |
| Spectral feature | λ_c [nm] | $\Delta\lambda$ [nm] | λ_e [nm] | $\Delta\lambda$ [nm] | |
| Spectral channels | 380 | 10 | 412 | 20 | 412.5 | 10 | 469 | 20 | 550 | 20 | 632 | 100 | |
| | 443 | 10 | 443 | 20 | 442.5 | 10 | 555 | 20 | 660 | 20 | 843 | 275 | |
| | 460 | 10 | 490 | 20 | 490 | 10 | 645 | 50 | 870 | 20 | | | |
| | 520 | 10 | 510 | 20 | 510 | 10 | 858.5 | 35 | | | | | |
| | 545 | 10 | 555 | 20 | 560 | 10 | | | | | | | |
| | 678 | 10 | 670 | 20 | 619 | 10 | | | | | | | |
| | 865 | 10 | 765 | 40 | 665 | 10 | | | | | | | |
| | | | 865 | 40 | 681.25 | 7.5 | | | | | | | |
| | | | | | 708.75 | 10 | | | | | | | |
| | | | | | 753.75 | 7.5 | | | | | | | |
| | | | | | 778.75 | 15 | | | | | | | |
| | | | | | 865 | 20 | | | | | | | |
| | | | | | 885 | 10 | | | | | | | |
| | | | | 900 | 10 | | | | | | | | |

λ_c : center wavelength; λ_e : effective wavelength; $\Delta\lambda$: spectral bandwidth

TABLE III
SATELLITE PASSING TIMES AND THE SENSOR'S SUN-OBSERVER
VIEWING GEOMETRY FOR APRIL 14, 2003

| UTC | Orbit | Satellite | Sensors | SunAZ [°] | SatAZ [°] | SunZ [°] | SatZ [°] |
|-------|------------|-----------|---------|-----------|-----------|----------|----------|
| 22:35 | Ascending | N16 | AHRR | 182.59 | 152.96 | 61.80 | 0.78 |
| 22:54 | Descending | Terra | MODIS | X | X | X | X |
| 22:57 | Descending | ADEOS-2 | GLI | 188.68 | 242.36 | 61.97 | 24.09 |
| 23:01 | Descending | Orbview-2 | SeaWiFS | 189.89 | 122.42 | 62.03 | 49.47 |
| 23:08 | Descending | ENVISAT | MERIS | 191.76 | 312.13 | 62.13 | 31.37 |
| 23:09 | Ascending | Aqua | MODIS | 192.02 | 255.86 | 62.14 | 34.58 |
| 23:33 | Descending | N17 | AHRR | 198.66 | 314.07 | 62.61 | 33.62 |

TABLE IV
SATELLITE PASSING TIMES AND THE SENSOR'S SUN-OBSERVER
VIEWING GEOMETRY FOR APRIL 26, 2003

| UTC | Orbit | Satellite | Sensors | SunAZ [°] | SatAZ [°] | SunZ [°] | SatZ [°] |
|-------|------------|-----------|-----------------|-----------|-----------|----------|----------|
| 21:41 | Descending | Terra | MODIS | 167.68 | 103.16 | 58.08 | 36.75 |
| 21:52 | Descending | ENVISAT | MERIS/ AATSR | 170.79 | 114.12 | 57.91 | 12.42 |
| 21:56 | Ascending | Aqua | MODIS | 171.93 | 59.63 | 57.86 | 15.00 |
| 22:57 | Descending | ADEOS-2 | GLI | 189.78 | 242.52 | 57.92 | 24.13 |
| 23:00 | Descending | Orbview | SeaWiFS | X | X | X | X |
| 23:19 | Descending | Terra | MODIS | 195.83 | 305.94 | 58.29 | 27.17 |

the apparent sunrise was at 14:17, the sunset at 6:40 (April 15th), solar noon at 22:26. For April 26, these values change slightly to 14:08 (apparent sunrise), 22:24 (solar noon), and 6:45 sunset at April 27. Note, that the 6S RTC is limited to 60° for viewing and 70° for solar zenith angles. Larger zenith or viewing angles may cause additional uncertainties due to plane parallel approximation of the atmosphere in the 6S code.

The CalVal site is located close to the Barrow observation site from the National Oceanic and Atmospheric Administration (NOAA). It is a horizontal field at the north slope of Alaska. For this approach, a site with a size of $2 \times 2 \text{ km}^2$ was selected having the center point at 71.31° N and 156.63° W . Additionally, a macro site of $5.6 \times 5.6 \text{ km}^2$ was used for uniformity check of the L1B data.

D. Calibration Coefficients

The comparison was mainly performed on the basis of TOA radiance or reflectance, depending on what kind of product was delivered by the different projects.

- *GLI* was in operational mode from April until October 2003. For the comparison, L1B data with prelaunch calibration factors were used. No further correction factors were applied, such as differences of the mirror sites or any degradation factors. Note, it was the objective of this analysis to check the radiometric performance of *GLI* in comparison with other space sensors.
- *MODIS (Terra)* was launched in December 1999, and the data were calibrated and validated recently. An overview of the performance is given in [7]. Whereas the Terra satellite is flown on a descending node during daytime, a similar instrument [*MODIS (Aqua)*] delivers daytime observation data in the ascending node. The Aqua satellite was launched in May 2002 [8].
- *MERIS/AATSR* are onboard the *ENVISAT*, which was launched in March 2002. At the time of the previous cross-calibration exercise [3], *MERIS* was in the commissioning phase. Now, *MERIS* and *AATSR* data products are considered to be calibrated and validated [9], [10].
- *SeaWiFS* has a much longer and rigorous calibration history, such as described in [11] for the direct methods and in [12] for the vicarious methods. *SeaWiFS* is an ocean color mission, and the calibration for ocean targets (dark signals) are retrieved vicariously over the Marine Optical Buoy (MOBY) site close to Hawaii. The vicarious calibration at MOBY is not applied to *SeaWiFS*'s land and cloud measurements. The calibration for these bright targets is retrieved via direct calibration methods, i.e., not vicariously. The *SeaWiFS* project does not deliver Level 1B data as a standard product. This is why Level 1A data were processed using the code SEADAS 4.4 (<http://seadas.gsfc.nasa.gov>). It delivers the required L1B data format as an optional output in TOA radiance.
- Also for the *AVHRR* sensors, there exists a long calibration history from early NOAA missions to the most recent NOAA-16 and NOAA-17 missions. The TOA reflectance and radiance for NOAA-16 were calculated using updated calibration coefficients provided by Heidinger *et al.* [6] recently. For NOAA-17, the prelaunch calibration factors were used (see http://orbitnet.nesdis.noaa.gov/crad/sit/page_of_pages.html). For the TOA radiance representation, the visible channel information for effective wavelengths, equivalent width, and solar irradiance based on [13] was used.

The L1B data (as TOA radiance) at the sensor crossing times during the April 14 calibration day (see Table III) are plotted versus center wavelength of each channel in Fig. 1.

E. Ground-Truth Data

The CalVal site is a large snow field in Alaskan tundra located about 5 km northeast of Barrow town and 2 km south of the NOAA's Climate Monitoring & Diagnostics Laboratory (CMDL).

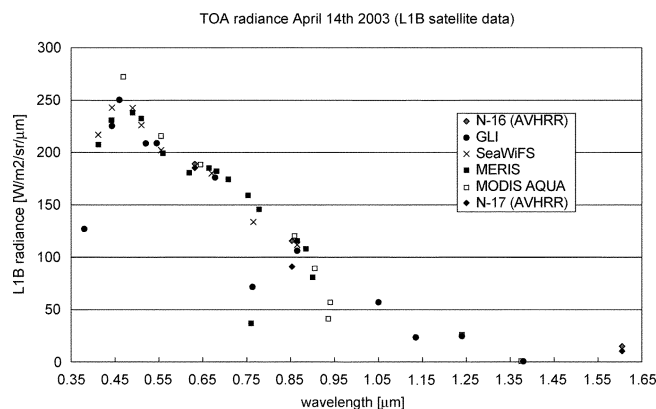


Fig. 1. TOA L1B data from *GLI*, *SeaWiFS*, *MERIS*, *MODIS (Aqua)*, and NOAA-16/17 data. TOA radiances at the CalVal site plotted versus center wavelength of each channel.

From April 11 until April 27, a CalVal campaign in the scope of the ADEOS-2 project was carried out. The site and the type of measurements performed at the site were described in detail recently [14], [15]. The results of this campaign are summarized in the following four parameters, which are relevant for this cross-calibration approach:

The CalVal site is a large horizontal flat snow field of $2 \times 2 \text{ km}^2$. The center point of the field is located at 71.31° N and 156.63° W ; additionally, a larger macro site ($5.6 \times 5.6 \text{ km}^2$) around the CalVal site was selected to perform uniformity checks of the satellite signal by comparing the TOA L1B of the CalVal site with those signals (and its deviation) retrieved from the macro site.

The spectral reflectance measurements were performed using an *FieldSpec FR* (Analytical Spectral Devices, Inc.). The reflectances of the selected days (April 14 and 26) differ slightly, caused by differences in the snow grain size. An average spectrum for each day's CalVal period was used as RTC input.

The AOT was retrieved using the measurements of a Prede "Skyradiometer." The AOT varies between the days, since the atmospheric conditions were different. Additionally, spectral reflectance and BRDF measurements on the ground were carried out. As shown in [15], the characteristics of a snow site are not entirely Lambertian over the entire spectral range. For the sun-observer viewing geometry during the satellite over flights (see Tables III and IV), no correction must be applied in the visible spectral range. In the NIR and shortwave infrared, corrections must be taken under consideration, especially regarding large viewing angles.

Additional local weather information and data from the U.S. Department of Energy's Atmospheric Radiation Measurement Program (ARM) and CMDL site was taken into account to intercompare and validate the measurement results performed at the CalVal site. An overview of the atmospheric conditions is given in Table V.

F. Algorithm

Both satellite and ground-truth data are input data for radiative transfer modeling. As RTC, a slightly modified version of the 6S code [4] was used. From the satellite data, the geolocation information, such as sun and viewing angles, is retrieved for each passing time of each satellite sensor.

TABLE V
OVERVIEW OF ATMOSPHERIC CONDITIONS ON
APRIL 14 AND 26 AT SOLAR NOON

| | Temperature [°C] | Humidity [%] | AOT @ 550 nm | H ₂ O [cm] | O ₃ [DU] | Pressure [hPa] |
|---------------|---------------------|-----------------|-----------------|--------------------------|------------------------|-------------------|
| April 14th | -5 | 93 | 0.0263 | 0.6 | 450 | 1002 |
| April 26th | -2 | 86 | 0.235 | 0.68 | 400 | 1025 |

The atmospheric input parameters for the RTC were defined using the AOT (measurements) and the aerosol components (assumptions) and taking additional atmospheric data into account (such as H₂O, ozone contents). For the aerosol components, a typical composition of 2.85% dust-like, 12.85% oceanic, 70% water-soluble components and 14.3% soot components was assumed [16] for the April 26. This composition could be confirmed with skyradiometer measurements at scattering angles of 5°, 7°, 10°, 15°, 20°, 25°, and 30°. However, measurements performed during April 14 showed a lower imaginary part of the refraction index, indicating that less absorbing aerosols could be found in the boundary layer. Using additional information from ARM Mircopulse Lidar (MPL) measurements, a thin homogenous cirrus layer could be identified. This nonvisible cirrus layer caused higher AOT, but since placed on the top of the boundary layer, the cirrus results in an offset in the TOA reflectance. However, the influence on the results for relative cross calibration is considered to be small, since the AOT measurements and MPL response (ARM measurements) were homogeneous during the observation time from 21:41 to 23:19. Also, the spectral influence of the cirrus is small, assuming constant spectral reflectance in the visible (ice cloud).

G. Results and Error Estimation

To provide an intersatellite comparison relatively to the space sensors under consideration, the ratio of L1B TOA to ground-truth modeled TOA data was calculated and plotted versus the center wavelength of each sensor channel.

Fig. 2 shows the result of this normalization for April 14 and 26, respectively. Keeping in mind that the error budget for each of the sensors is in the range of 5% and that the method has an inherent error of 5% for a single comparison, all satellite sensor L1B data are in the limits of the error bars.

However, the following tendency becomes obvious. GLI's performance is encouraging at this early point of the mission (GLI was operational from April 2003). There is an excellent agreement in the visible (channels 7, 8, and 13). Channel-1 and Channel-19 seem to be too low; however, the deviation between the calibration days is significant.

For the other space sensors, the following tendency becomes "interesting": when looking at Fig. 2: MODIS Aqua, AATSR, and AVHRR Channel-1 are located at the upper limit of the range and MODIS Terra (together with GLI) are at the lower limit. MERIS and SeaWiFS seem to have a similar performance (with MERIS a bit higher than SeaWiFS) and are located in the center of the range. AVHRR Channel-2 is more difficult to assess, since this channel has a broad spectral bandwidth ($\Delta\lambda > 200$ nm) in a spectral region where snow reflectance is decreasing.

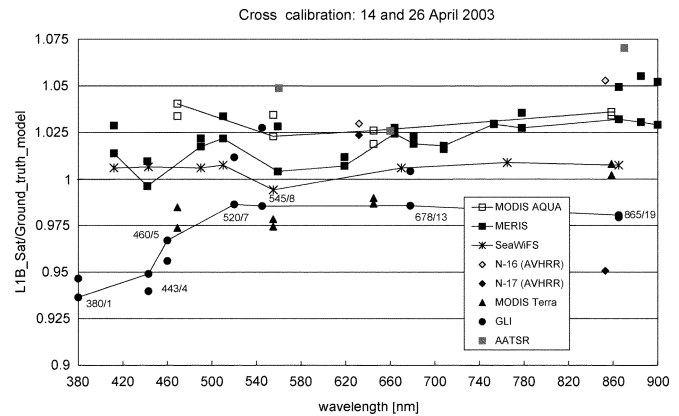


Fig. 2. Ratio of L1B satellite data and vicariously calculated TOA data using ground-truth measurements for April 14/26, 2003. For GLI channels, also the center wavelength and the channel number are indicated. GLI, MERIS, MODIS (Aqua), and SeaWiFS for the April 14 datasets are indicated in solid lines.

H. Accuracy of the Method

The accuracy of a single satellite intercalibration depends mainly on the accuracy of the space sensor (4% to 5%), which will be used as a reference calibration source. Further uncertainties are measurement accuracy (e.g., uniformity of the site, positioning accuracy) and uncertainties from atmospheric modeling and assumptions (e.g., change of atmospheric conditions, atmospheric characterization, and correction for viewing angle differences). Hence, the rms error of a single intersatellite comparison is in the range of 5% to 6.6%. Assuming this error budget, all 12 L1B datasets used in this satellite intercalibration are within the error bars of the sensors' calibration accuracies and the uncertainties of this vicarious calibration approach.

III. CONCLUSION

For the 12 datasets, this comparison showed that all TOA radiances are within the error bars of the sensors' calibration accuracies and the uncertainties of this vicarious calibration approach. However, a tendency in the datasets was recognized: GLI and MODIS (Terra) seem to slightly underestimate the snow site, and AATSR, MODIS (Aqua), and AVHRR upel-1 are slightly overestimating the same site. In the center, SeaWiFS and MERIS are close to the predicted TOA values, whereas MERIS seems slightly higher than SeaWiFS. AVHRR Channel-2 is difficult to assess, since the channel has a broad spectral bandwidth of $\Delta\lambda > 200$ nm.

Concluding, it was an encouraging result for GLI at that point of the mission. Using the prelaunch calibration factors, GLI delivers comparable results to other space sensor in the visible and near infrared.

These results are currently compared with other CalVal technique results, such as the onboard (solar, lamp) and vicarious (e.g., desert sites, ocean sites) calibration, such as described in [17]–[19]. This ongoing comparison will deliver a better understanding of GLI's performance and the limitations of the various CalVal techniques.

ACKNOWLEDGMENT

The authors would like to thank the National Aeronautics and Space Administration's SeaWiFS Project, Distributed Active Archive Center, B. Holben (PI Aeronet site at Barrow), C. R. McClain (SeaDAS code), E. Vermote (6S code), the European Space Agency, Brockmann Consulting, U.S. Department of Energy, and NOAA's Satellite Active Archive and Climate Monitoring and Diagnostics Laboratory for the production and distribution of data and codes used in this letter, respectively.

The authors want also to express their appreciation for considerable help of the GLI calibration-working group (leader: Y. Senga) and the ADEOS-2 project team. Last but not least, the authors would like to acknowledge the support and help from various collaborators, such as R. Storvold, H. Eide, Y. Iizuka, and Y. Nakajima.

REFERENCES

- [1] T. Y. Nakajima, T. Nakajima, M. Nakajima, H. Fukushima, M. Kuji, A. Uchiyama, and M. Kishino, "Optimization of the Advanced Earth Observing Satellite (ADEOS) II Global Imager (GLI) channels by use of radiative transfer calculations," *Appl. Opt.*, vol. 37, no. 15, pp. 3149–3163, 1998.
- [2] IOCCG, "Remote sensing of the ocean color in coastal, and other optically-complex waters," IOCCG, Dartmouth, NS, Canada, IOCCG Rep. 3, Reports of the International Ocean-Color Coordinating Group, S. Sathyendranath, Ed., 2000.
- [3] J. Nieke, M. Hori, R. Höller, I. Asanuma, and T. Aoki, "Satellite sensor inter-calibration; a case study," in *Proc. ENVISAT Validation Workshop*, Frascati, Italy, Dec. 9–13, 2003, http://envisat.esa.int/workshops/validation_12_02/proceedings/meris/06_nieke.pdf, pp. 1–10.
- [4] E. Vermote, D. Tanre, J. L. Deuze, M. Herman, and J. J. Morcrette, "Second simulation of the satellite signal in the solar spectrum '6S': An overview," *IEEE Trans. Geosci. Remote Sensing*, vol. 35, pp. 675–686, May 1997.
- [5] G. Thuillier, M. Herse, D. Labs, T. Foujols, W. Peetermans, D. Gillotay, P. C. Simon, and H. Mandel, "The solar spectral irradiance from 200 to 2400 nm as measured by the SOLSPEC spectrometer from the ATLAS and EURECA missions," *Solar Phys.*, vol. 214, pp. 1–22, 2003.
- [6] A. Heidinger, C. Cao, and J. Sullivan, "Using MODIS to calibrate AVHRR reflectance channels," *J. Geophys. Res.*, vol. 107, no. D23, p. 4702, 2002.
- [7] B. Guenther, X. Xiong, V. Salomonson, W. Barnes, and J. Young, "On-orbit performance of the earth observing system moderate resolution imaging spectroradiometer; first year of data," *Remote Sens. Environ.*, vol. 83, pp. 16–30, 2002.
- [8] X. Xiong, V. Chiang, J. Sun, and W. Barnes, "Aqua MODIS first year on-orbit calibration and performance," *Proc. SPIE*, vol. 5234, 2003.
- [9] D. Smith, "AATSR 1st year calibration results," in *Working Meeting MERIS and AATSR Calibration and Geophysical Validation (MAVT-2003) ESRIN*, Frascati, Italy, Oct. 20–24, 2003.
- [10] S. Delwart, L. Bourg, and J. Huot, "MERIS 1st year: Early calibration results," *Proc. SPIE*, vol. 5234, 2003.
- [11] R. A. Barnes, R. E. Eplee, G. M. Schmidt, F. S. Patt, and C. R. McClain, "The calibration of SeaWiFS. I direct techniques," *Appl. Opt.*, vol. 40, pp. 6682–6700, 2001.
- [12] R. E. Eplee, W. D. Robinson, S. W. Bailey, D. K. Clark, P. J. Werdell, M. Wang, R. A. Barnes, and C. R. McClain, "The calibration of SeaWiFS. II vicarious techniques," *Appl. Opt.*, vol. 40, pp. 6701–6718, 2001.
- [13] H. Neckel and D. Labs, "The solar radiation between 3300 and 12500 Å," *Solar Phys.*, vol. 90, pp. 205–258, 1984.
- [14] T. Aoki, T. Aoki, M. Fukabori, Y. Tachibana, Y. Zaizen, F. Nishio, and T. Oishi, "Spectral Albedo observation on the snow field at Barrow, Alaska," *Polar Meteorol. Glaciol.*, vol. 12, pp. 1–9, 1998.
- [15] T. Aoki, T. Aoki, M. Fukabori, A. Hachikubo, Y. Tachibana, and F. Nishio, "Effects of snow physical parameters on spectral albedo and bidirectional reflectance of snow surface," *J. Geophys. Res.*, vol. 105, no. D8, pp. 10219–10236, 2000.
- [16] S. Ohta, private communication, 2003.
- [17] H. Murakami, K. Tanaka, S. Kurihara, Y. Okamura, J. Inoue, J. Nieke, I. Asanuma, H. Yatagai, Y. Mitomi, M. Yoshida, R. Higuchi, S. Kawamoto, K. Isono, and Y. Senga, "GLI early calibration results for oceanographic applications," *Proc. SPIE*, vol. 5155, 2003.
- [18] M. Yoshida, Y. Mitomi, Y. Senga, H. Murakami, I. Asanuma, S. Kurihara, K. Sasaoka, and K. Sato, "Early phase evaluations of GLI vicarious calibration factors for ocean color channels," *Proc. SPIE*, vol. 5155, 2003.
- [19] J. Nieke, K. Tanaka, N. Itoh, T. Kimura, and S. Kurihara, "First results from GLI's solar calibration," *Proc. SPIE*, vol. 5151, pp. 415–423, 2003.